Journal of Laser Applications

RESEARCH ARTICLE | OCTOBER 16 2025

# Surface modification by combining extreme high-speed laser material deposition (EHLA) with simultaneous roller burnishing

**Special Collection:** 9th International Congress on Laser Advanced Materials Processing

Viktor Glushych ✉ ; Kim Kallies ; Max Zimmermann ; Harald Betsch ; Bodo Vieland ; Christian Henk ; Thomas Schopphoven ; Wilhelm Meiners



*J. Laser Appl.* 37, 042026 (2025)
https://doi.org/10.2351/7.0001861

Journal of Laser Applications ARTICLE pubs.aip.org/lia/jla

# Surface modification by combining extreme high-speed laser material deposition (EHLA) with simultaneous roller burnishing

Cite as: J. Laser Appl. 37, 042026 (2025); doi: 10.2351/7.0001861
Submitted: 6 June 2025 · Accepted: 30 September 2025 ·
Published Online: 16 October 2025



Viktor Glushych,[1,2,a)] Kim Kallies,[1] Max Zimmermann,[1] Harald Betsch,[3] Bodo Vieland,[4] Christian Henk,[4] Thomas Schopphoven,[1] and Wilhelm Meiners[1]

## AFFILIATIONS

[1]Fraunhofer Institute for Laser Technology ILT, 52074, Aachen, Germany
[2]RWTH Aachen University, Chair for Laser Technology LLT, Steinbachstraße 15, 52074 Aachen, Germany
[3]Liebherr-Aerospace Lindenberg GmbH, 88161, Lindenberg, Germany
[4]Hegenscheidt-Mfd GmbH, 41812, Erkelenz, Germany

**Note:** This paper is part of the Special Topic on the 9th International Congress on Laser Advanced Materials Processing.
[a)]**Author to whom correspondence should be addressed; electronic mail:** viktor.glushych@ilt.fraunhofer.de



## ABSTRACT

This study investigates the fundamentals of the simultaneous coating and roller burnishing process as a novel approach for improving the surface and subsurface properties of EHLA-deposited material. The combination of EHLA and roller burnishing yields significant improvements in surface roughness, microhardness, and residual stress distribution. The residual heat from the EHLA process was observed to increase surface plasticity during simultaneous processing, significantly influencing the effectiveness of roller burnishing as a function of the tool center point (TCP) offset parameter $\Delta z$. Surface finish is most favorably affected at a moderate $\Delta z$ of 4 mm, suggesting the existence of an optimal thermal window for surface smoothing. The highest hardness was achieved at the smallest offset ($\Delta z = 1$ mm), potentially due to precold deformation effects and stress-assisted martensitic transformation. In terms of residual stress modification, all burnishing strategies succeeded in transforming high subsurface tensile stresses into beneficial compressive stresses, which are expected to enhance bending fatigue performance. The TCP offset further allowed directional stress control, enabling differentiated axial and circumferential stress profiles. Further studies are required to explore the relationship between the observed residual stress profiles and the corresponding fatigue resistance of repaired components under service-relevant loading conditions.

Key words: EHLA, roller burnishing, simultaneous, tensile stress, compressive stress, DED-LB/P, 300M, repair, aircraft, landing gear



## I. INTRODUCTION

Extreme high-speed laser material deposition (EHLA) is recognized as a highly productive and resource-efficient advancement over conventional laser material deposition (LMD or DED-LB), used for coating, repair, and additive manufacturing of components.[1,2] Although EHLA achieves notable surface quality compared to LMD, mechanical postprocessing of the deposited layers often remains necessary, representing a considerable time and cost constraint. In this context, the combination of additive and subtractive manufacturing processes has gained growing attention in recent years. A notable example is the simultaneous machining and coating (SMaC) process, developed by Fraunhofer ILT, which combines EHLA and turning into a single step, demonstrating improved productivity and surface quality alongside reduced tool wear.[3] Another compelling yet unresearched method is the combination of EHLA with simultaneous roller burnishing. In this approach, the roller burnishing tool interacts with the component during the EHLA coating process, maintaining a predetermined horizontal offset between the tool center points (TCPs), denoted as $\Delta z$ (Fig. 1). By employing plastic deformation rather than material

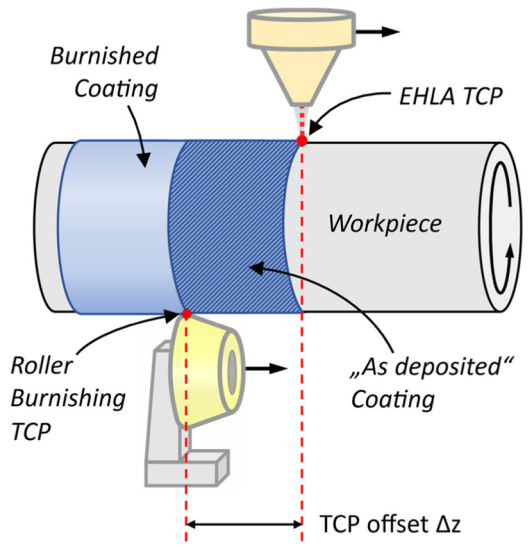


**FIG. 1.** Operating principle of SCaRB and definition of TCP offset Δz.

removal, this technique not only has the potential to enhance the surface quality but also influences the microstructure, residual stress, and mechanical properties of the deposited and surrounding material.

Roller burnishing and deep rolling, among other surface treatment methods like shot peening, hammering, and ultrasonic impact treatments, enhance surface properties by applying a specific pressure on the surface of a component, causing a controlled deformation, strain hardening, and inducing controlled residual stresses.[4,5] The combination of elastic and plastic deformation mechanisms results in improved surface roughness, surface densification, and the induction of beneficial residual compressive stresses. While deep rolling primarily aims to enhance fatigue strength and component lifetime by introducing stresses at depths reaching up to 4 mm or more,[6] roller burnishing is primarily employed to refine surface properties, with its mechanical effects typically limited to a depth of a few hundred micrometers.[7]

Despite its primary function in surface smoothing and enhancing wear and corrosion resistance, roller burnishing also modifies the near-surface residual stress profile, which can enhance fatigue performance and inhibit crack initiation and propagation.[8] Common applications of roller burnishing include crankshafts, train axles, and landing gear components.[9–11] For many of these applications, dedicated deep rolling or burnishing machines is typically employed in industrial settings. However, roller burnishing tools can also be adapted for use on conventional computer numerical control lathes, offering increased process flexibility.

In a recent study, Liu *et al.*[12] explored the parallelization of conventional LMD and plastic deformation by rolling, applying the approach to the deposition of a high-entropy alloy on a flat steel substrate. The study revealed that *in situ* rolling (ISR) significantly alters microstructural evolution, refining the columnar grain morphology into equiaxed grains and reducing grain size by up to 68%. Comprehensive analysis of the processed coatings revealed that ISR could reduce porosity, while enhancing surface quality and microhardness, leading to improved resistance to adhesive and abrasive wear.

Landing gear systems are among the most highly stressed structural components of an aircraft, enduring high mechanical loads and harsh environmental conditions throughout the aircraft service cycle. These components are highly cost-intensive due to the use of specialized aerospace-grade materials, the complexity of involved manufacturing processes, and the requirement for advanced surface treatments to ensure their wear and corrosion resistance. Despite all the efforts made to meet the requirements, regular inspections repeatedly reveal worn and/or damaged areas that need to be repaired.[13,14] Unscheduled replacement with new parts is impractical due to high lead times and costs involved. While SAE AIR 5885[15] outlines standard procedures for maintaining and repair of landing gear components, it does not yet address additive repair techniques, such as LMD or EHLA, for the restoration of worn or corroded material.

For repair procedures outside the scope of the SAE guide, comprehensive validation and substantiation are required. Establishing reliable additive repair methods for high-strength alloys like 300M is crucial to enable extended repair capabilities in landing gear applications. EHLA has emerged as a particularly favorable technique for this purpose due to its ability to produce dense, metallurgically bonded coatings with minimal thermal impact on the workpiece. However, any laser-based deposition process is accompanied by a change in the microstructure of the substrate and residual stress conditions, which can have a negative effect on the mechanical properties, such as fatigue behavior, and, thus, entail the risk of premature failure.

The combination of EHLA with simultaneous roller burnishing presents a promising approach for mitigating detrimental residual tensile stresses and modifying the dendritic structures in deposited material. Ultimately, this process combination may offer a viable pathway for the repair of worn or corroded areas on landing gear components, enabling restoration to their original specifications or even enhancing their properties beyond initial state. This would significantly enhance sustainability, cost-efficiency, and operational resilience by enabling the reuse of highly stressed, safety-critical aerospace components, while also aligning with the European circular economy action plan.

In this study, the novel simultaneous coating and roller burnishing (SCaRB) process is investigated as a method to modify the surface and mechanical properties of EHLA depositions, focusing on the coating and repair of aircraft landing gear components. SCaRB utilizes residual heat from laser deposition to enhance plastic deformation during burnishing while allowing control over induced stresses through adjustment of the tool offset and variation of roller tool radius. In analogy to the SMaC approach, this combination is achievable due to the close alignment of surface velocities between the two processes. This work focuses on the parallelization of the two subprocesses and the evaluation of surface pressure exerted by the burnishing tool, along with TCP offset, as key parameters influencing the mechanical properties and surface quality of the deposited material. The suggested method offers potential in mitigating tensile stresses induced through the

deposition process[16] which are particularly challenging for aerospace components subjected to bending loads.

## II. MATERIALS AND METHODS

### A. Handling system

Simultaneous processing requires a customized system capable of integrating EHLA and roller burnishing within a single setup. A machine fulfilling these criteria was developed through a collaboration between the Fraunhofer Institute for Laser Technology ILT and J.G. Weisser Söhne, based on the Weisser ARTERY M-2 TM mill-turn center (Fig. 2).

The beam source utilized for the EHLA process is a Laserline LDF 8000-30 diode laser with a maximum output power of 8.7 kW and a beam quality of 30 mm × mrad. The beam is focused on the workpiece surface by a Laserline OTZ-5 zoom optic, which generates a circular top-hat profile with a variable spot diameter between 1.4 and 4.6 mm. Powder is supplied using an Oerlikon Metco Twin 150 volumetric feeder, delivering the material through a HighNo 4.0 continuous coaxial EHLA nozzle from HD Sonderoptiken. The machine's main spindle achieves rotation speeds up to 5700 rpm and is capable of handling workpieces with lengths up to 1000 mm.

A bespoke roller burnishing tool, developed by Hegenscheidt-Mfd, was implemented into the modified ARTERY M-2 platform using the machine turret's BMT 65 interface to enable mechanical surface processing. In the existing configuration, the TCP of the roller burnishing tool is positioned opposite to that of the laser TCP, relative to the component's rotational axis. The roller burnishing tool assembly incorporates an internal disk spring stack. The applied burnishing force is altered by adjusting the number and configuration of these springs. Exchangeable rollers with a roller diameter of ~65 mm and varying roller edge radii ($R = 3.5$ mm and $R = 7.5$ mm) allow for controlled adjustment of the contact area and the resulting Hertzian pressure.

### B. Substrate and powder material

300M tubes in hardened condition with dimensions of 240 mm in length, 80 mm in outer diameter, and 15 mm wall thickness served as substrate material in the experiments. To replicate the operational surface condition of landing gear components, the substrates underwent shot peening followed by precision grinding. Commercially available AISI 4340 powder with a particle size distribution of 15–53 $\mu$m (GKN Hoeganaes) was selected as the EHLA feedstock material. With 300M being a modified variant of AISI 4340, the chemical makeup of both materials is comparable. Nominal compositions are detailed in Table I.

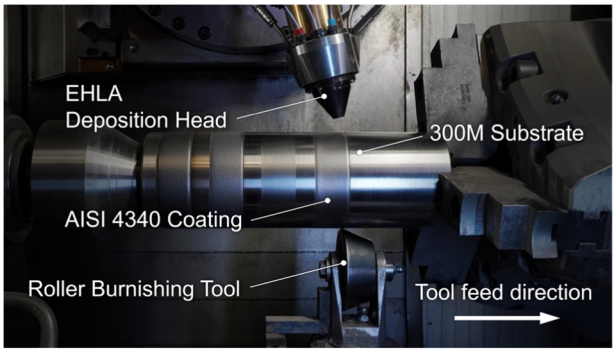


**FIG. 2.** Experimental setup for SCaRB on a modified Weisser ARTERY M-2 TM.

**TABLE I.** Chemical composition of the substrate and powder materials used in the experimental work.

| Material | Fe | Ni | Cr | Si | Mn | Mo | C |
|---|---|---|---|---|---|---|---|
| 300M substrate | Bal. | 1.8 | 0.82 | 1.6 | 0.8 | 0.4 | 0.42 |
| AISI 4340 | Bal. | 1.9 | 0.9 | 0.3 | 0.8 | 0.2 | 0.41 |

### C. Experimental approach

To systematically study the influence of simultaneous and sequential roller burnishing on surface quality, induced residual stress, and resulting microhardness, a total of 15 SCaRB experiments were carried out. The experimental matrix included variations of the following parameters:

- Number of deposited EHLA layers ($N = 0$; $N = 1$; $N = 3$).
- Burnishing strategy (no burnishing; simultaneous at $\Delta z = 1$ mm; simultaneous at $\Delta z = 4$ mm; sequential burnishing).
- Roller edge radius of the burnishing tool ($R = 3.5$ mm; $R = 7.5$ mm).

EHLA process parameters were held constant across all trials. The corresponding parameter set was iteratively developed prior to the main experimental campaign and is summarized in Table II. To minimize the risk of systematic errors, the sequence of experiments was randomized. To prevent contamination of the coating surface due to powder adhesion prior to roller burnishing, the EHLA deposition head was inclined by 15° in the feed direction. A uniform burnishing force of 4.5 kN was maintained across all burnishing strategies and for both tool radii, with the setup controlled via a dial gauge and monitored using a load cell. In all experiments, the feed rate of the roller burnishing process was matched to that of the EHLA deposition process at 0.3 mm/rev. The length of each deposited and/or burnished segment was fixed at 25 mm. In the sequential roller burnishing strategy, a dwell time was introduced between the coating and burnishing steps to allow the deposited

**TABLE II.** EHLA process parameters for the experimental trials.

| Parameter | Unit | Value |
|---|---|---|
| Surface speed | m/min | 50 |
| Laser power | W | 3480 |
| Laser spot Ø | mm | 2.43 |
| Powder mass flow | kg/h | 1.65 |
| Feed rate | mm/rev | 0.3 |

material to cool below 50 °C under ambient conditions prior to further processing, verified with a thermocouple. The same dwell time was applied between each deposition pass in the multilayer experiments. Each layer in the multilayer experiments was subjected to a roller burnishing step, both in simultaneous and sequential processing strategies.

### D. Evaluation methodology

The evaluation of fabricated samples included acquisition of residual stress profiles, metallographic analysis, and microhardness measurement, as well as optical surface characterization.

Residual stress was quantified using x-ray diffraction analysis of anisotropic lattice deformation in accordance with DIN EN 15305. Measurements were performed at the center of the coated and burnished region on unsectioned samples, using nominal depth increments of 50 $\mu$m to a maximum depth of 750 $\mu$m below the surface. The defined measurement depths were achieved through controlled electrolytic etching and subsequently verified using a calibrated dial gauge. The process yields a consistent measurement uncertainty of 3 $\mu$m across the evaluated depth profile. An Xstress DR45 diffractometer and Xstress Studio software was used for the analysis applying the $\sin^2\psi$ method with $CrK_\alpha$ radiation ($\lambda = 0.2291$ nm). Residual stress measurements were conducted in both the circumferential and axial directions.

Following residual stress characterization, the samples were mechanically sectioned, mounted in resin, ground, etched with Nital, and analyzed via light microscopy. HV0.2 microhardness profiles were acquired using a QATM Qness 60 A+ Vickers hardness tester along the cross section.

The roughness of deposited and/or roller burnished surfaces was measured by white light interferometry using a Zygo Ametek NX2 system. Curvature correction was performed via cylindrical fitting using Zygo Mx 7.3 software, with further data analysis carried out in MountainsMap 7.4. The roughness values were extracted from roughness profiles according to DIN EN ISO 4288:1998 and DIN EN ISO 4287. To obtain statistically representative results, five surface profiles were acquired per sample.

## III. RESULTS

### A. Microstructure and surface roughness

Representative cross sections of AISI 4340 coatings deposited on 300M substrates are shown in Fig. 3. While all coatings exhibit localized small-scale lack-of-fusion defects, the optical analysis reveals no indications of cracking, delamination, or significant pore formation. Single-layer coatings have an average thickness of $160 \pm 30$ $\mu$m, increasing to $470 \pm 50$ $\mu$m for three layers. The heat-affected zone (HAZ) remains uniform at approximately 100 $\mu$m across all samples. Notably, a tempered microstructure is observed in the lower part of multilayer coatings, indicative of cumulative thermal cycling during successive deposition passes.

A top view of selected single-layer EHLA coatings is provided in Fig. 4. Figure 4(a) illustrates a coating in the "as deposited" state, showing a characteristic waviness profile without an apparent periodic structure along the rotational axis, confirming the absence of

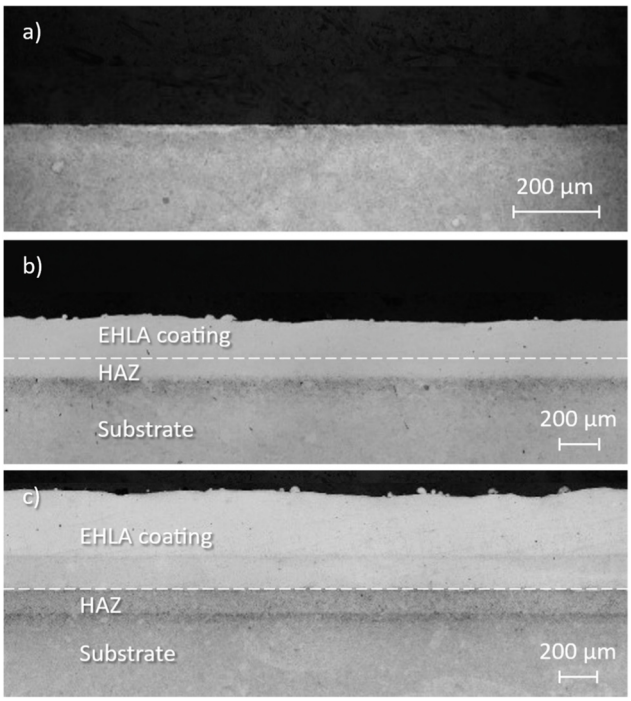


**FIG. 3.** Cross-sectional microscopy of etched substrate and "as deposited" coatings: (a) uncoated substrate, (b) single-layer EHLA deposition, and (c) three-layer EHLA deposition.

roller burnishing post-treatment. Figure 4(b) illustrates a coating subjected to sequential roller burnishing. While an overall smoothing of the surface is evident, the characteristic morphological features of the EHLA process are clearly retained. In contrast, Fig. 4(c) presents a SCaRB coating generated with a tool offset of $\Delta z = 1$ mm. This surface exhibits distinct, fine axial rifling, with the periodicity of the features corresponding to the axial feed of the roller burnishing tool. The typical surface topography associated

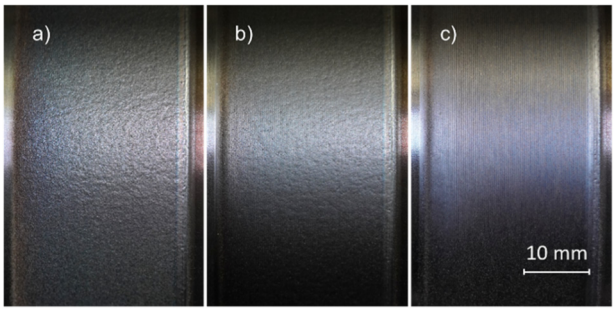


**FIG. 4.** Images of single-layer AISI 4340 EHLA coatings: (a) as deposited, (b) coating after sequential burnishing, and (c) simultaneous burnishing with $\Delta z = 1$ mm.

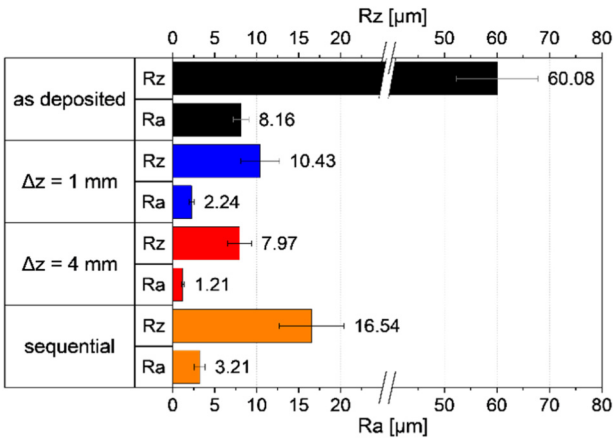


**FIG. 5.** Surface roughness of three-layer coatings subjected to simultaneous ($\Delta z = 1$ mm and $\Delta z = 4$ mm), sequential, and no roller burnishing ("as deposited").

with EHLA is no longer observable and indicates an enhanced plastic deformation of the surface due to residual heat from the coating process. These initial qualitative observations are supported by surface roughness data obtained through white light interferometry, as illustrated in Fig. 5.

The surface roughness of the three-layer "as deposited" coating, characterized by average roughness $Ra = 8.16\,\mu m$ and mean roughness depth $Rz = 60.08\,\mu m$, aligns well with previously published data.[3,17] As expected, a noticeable improvement in surface roughness is observed for EHLA coatings undergoing a roller burnishing treatment. The sequential strategy yielded a 72.5% decrease in Rz and 60.7% in Ra compared to the unprocessed condition. Even greater improvements were achieved using both simultaneous strategies, with the $\Delta z = 4$ mm configuration even reaching reductions of 85.2% in Ra and 86.7% in Rz.

## B. Microhardness

Figure 6 displays the microhardness depth profiles for the three-layer AISI 4340 coatings achieved under different roller burnishing conditions using the $R = 3.5$ mm tool. The surface-near region (0–300 $\mu$m) consistently demonstrates the highest and most uniform hardness values. In the "as deposited" state, this section of the EHLA coating shows an average hardness of 644 HV. Application of roller burnishing, regardless of strategy, results in a significant increase in near-surface microhardness. The most substantial increase is observed with simultaneous burnishing conducted at a TCP offset of $\Delta z = 1$ mm, reaching up to 722 HV—a ~12% improvement over the "as deposited" state. With sequential burnishing strategy, a ~6.5% increase in hardness was achieved. Below this near-surface region, a steep gradient is evident, with hardness declining to 400–500 HV at a depth of ~350 $\mu$m. This drop is attributed to the thermal cycling effects inherent in the multilayer deposition process, which induces partial tempering of the heat-affected and previously deposited layers and aligns with findings from previous work from Li *et al.* on EHLA of AISI 4340.[18]

## C. Residual stress

Figure 7 illustrates the influence of different burnishing strategies and varying tool roller radii on the circumferential and axial residual stress profiles of three-layer AISI 4340 repair coatings. A distinct contrast is observed between the "as deposited" condition and the roller burnished states. In the untreated EHLA coating, a shallow compressive residual stress zone is present in the upper 300 $\mu$m, followed by a sharp transition to high tensile stresses at greater depths. Peak tensile stress values reach approximately 1200 MPa in the circumferential direction and 800 MPa in the axial



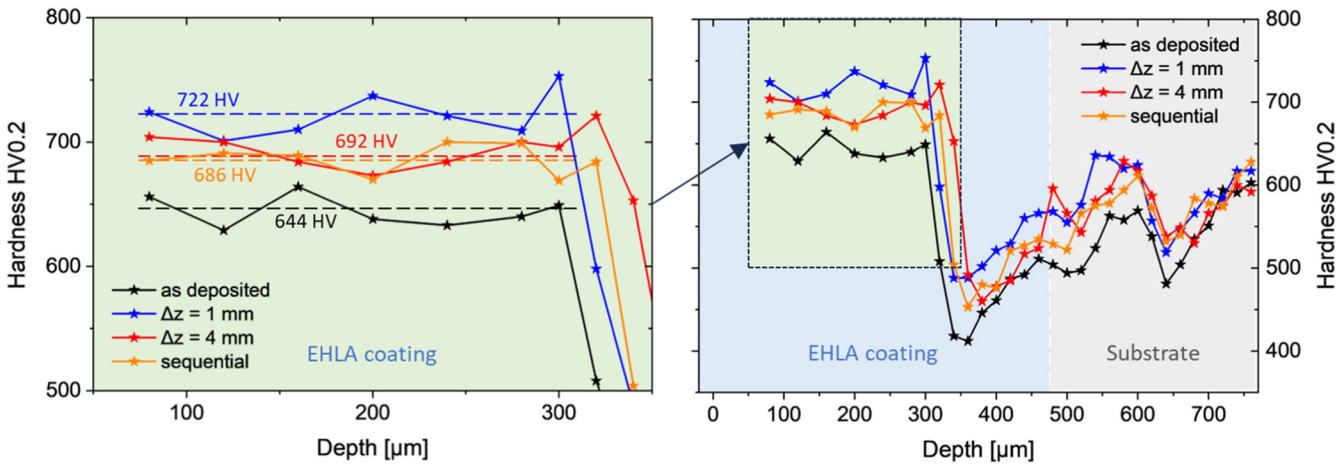


**FIG. 6.** Comparison of Vickers hardness depth profiles in multilayer EHLA coatings under "as deposited," simultaneous burnishing ($\Delta z = 1$ mm and $\Delta z = 4$ mm), and sequential burnishing conditions.

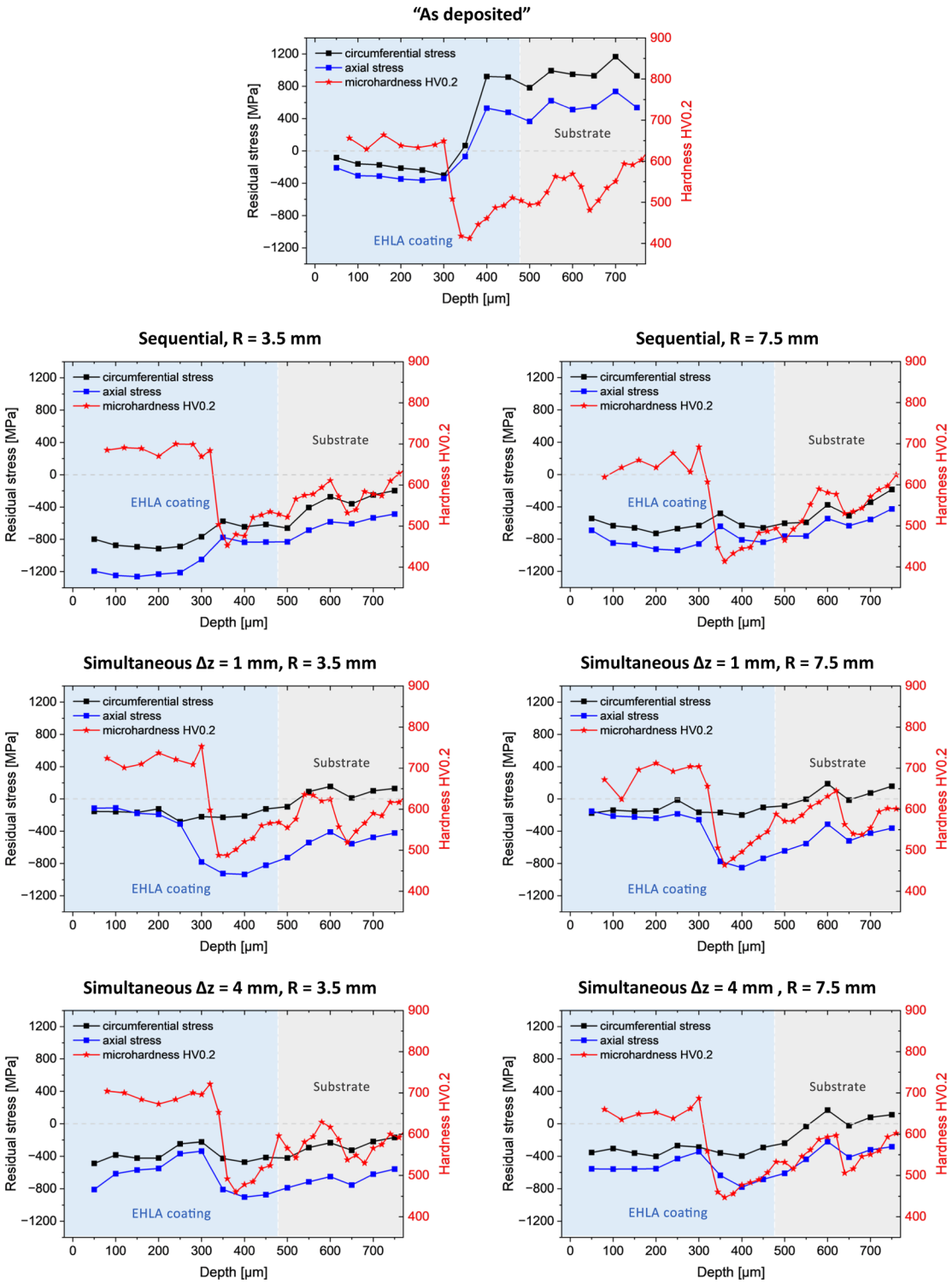


**FIG. 7.** Comparison of residual stress profiles in multilayer EHLA coatings under "as deposited," simultaneous ($\Delta z = 1$ mm and $\Delta z = 4$ mm), and sequential burnishing conditions for different burnishing roller edge radii ($R = 3.5$ mm and $R = 7.5$ mm).

direction. The presence of critical tensile residual stresses beneath the surface of the deposited material significantly compromises the bending fatigue strength of the component and poses a challenge for the intended repair application. Under high bending load, damage initiation has been shown to occur in this subsurface region, as demonstrated by Li *et al.*[16]

Under the selected processing parameters, sequential burnishing applied to cooled coating samples effectively shifts the entire residual stress profile into a compressive domain across both measured directions. Axial and circumferential compressive residual stresses peak at values beyond −800 and −1200 MPa, respectively. This approach not only neutralizes the tensile stresses associated with EHLA deposition but also moderates the stress gradient, reducing the risk of damage from abrupt subsurface stress transitions.

The residual stress profiles generated with roller burnishing tools with $R = 3.5$ mm and $R = 7.5$ mm exhibit a similar characteristic pattern, although peak values differ notably. The samples processed with the larger-radius tool ($R = 7.5$ mm) consistently exhibit lower peak compressive residual stresses and reduced surface hardness. This outcome is consistent with theoretical expectations. Given the identical burnishing force, a larger tool radius results in a greater contact area and a lower Hertzian contact pressure, which in turn induces less plastic deformation, reduced dislocation density, and consequently leads to lower residual stresses and hardness.[19]

As evident from the superimposed profiles in Fig. 8, the sequential burnishing strategy consistently results in the highest compressive residual stresses near surface, independent of the roller edge radius employed. This is followed by the simultaneous burnishing strategy with a TCP offset of $\Delta z = 4$ mm. In contrast, when the TCP offset is reduced to $\Delta z = 1$ mm, placing the burnishing tool in immediate proximity to the EHLA deposition zone, the resulting circumferential stress profile extends horizontally alongside the neutral stress axis ($0 \pm 200$ MPa). This behavior is attributed to the influence of residual heat from the EHLA process, which appears to facilitate localized stress relief, effectively neutralizing both compressive and tensile components.

A distinctive feature of the simultaneous burnishing process emerges in the axial residual stress profiles. Whereas the circumferential and axial residual stress distributions in both the "as deposited" and sequentially burnished coatings remain largely consistent throughout the measured depth (see Fig. 7), the axial stress profile of the simultaneously burnished repair volumes follows this trend only down to approximately 300 $\mu$m, beyond which it exhibits a

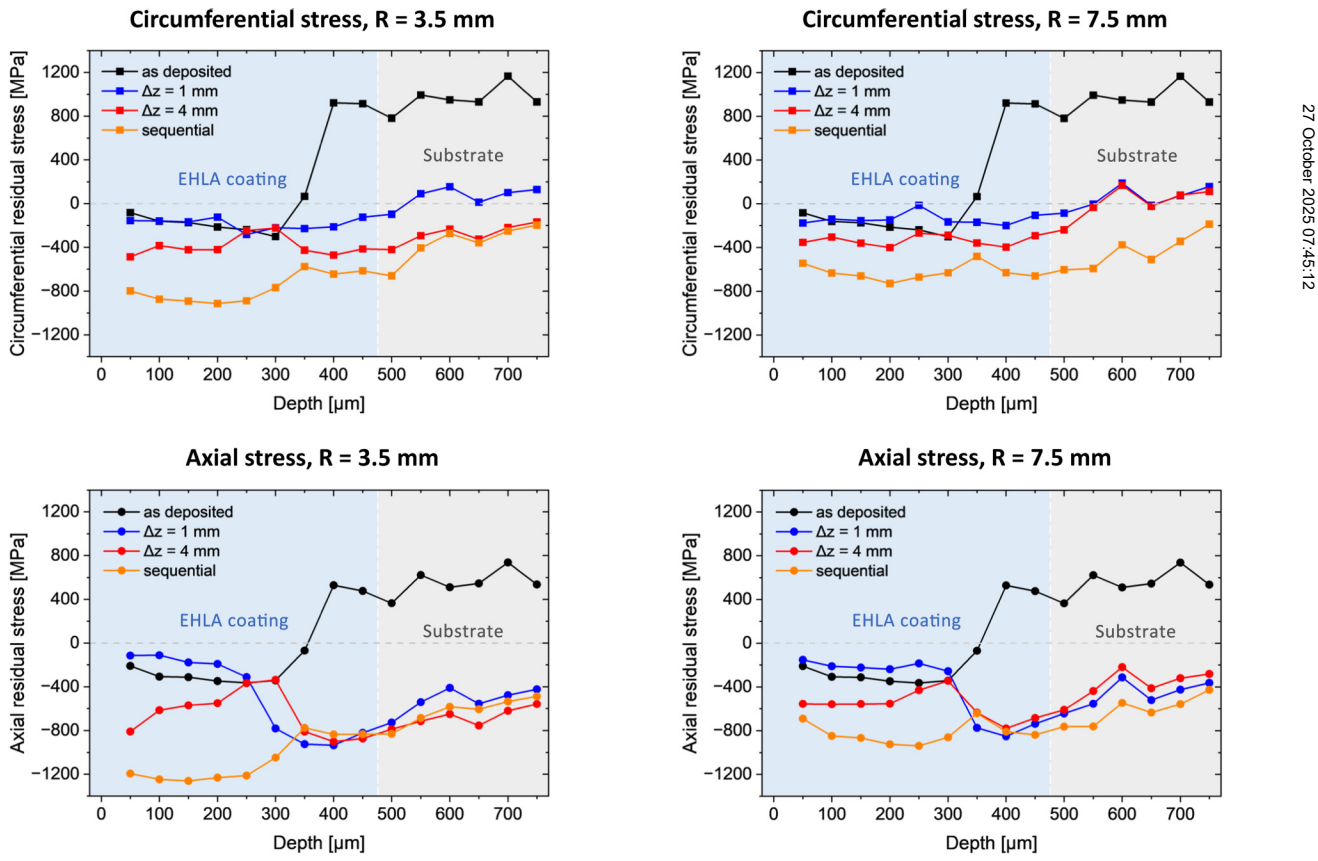


**FIG. 8.** Compiled overview of EHLA and SCaRB stress profiles categorized by circumferential and axial stress directions.

pronounced transition into the compressive regime. Although axial stress amplitude can be adjusted via axial feed variation, the ability to decouple axial and circumferential stress evolution while maintaining a constant feed appears to be a distinctive characteristic of the simultaneous burnishing method employed in this work. Although further research is necessary to provide a complete understanding of the governing mechanisms, a preliminary explanatory hypothesis can be proposed based on experimental observations.

As shown in Fig. 7, a distinct shift in both microhardness and axial residual stress profiles consistently occurs at a depth of ~300 $\mu$m across all analyzed samples. The observed discontinuity cannot be linked to the coating–substrate interface, given that it lies entirely within the deposited region in multilayer samples, and within the substrate in single-layer coatings. This location invariance points to a process-driven cause rather than a material boundary. Additionally, the fact that this anomaly occurs independently of the roller radius and is present even in "as deposited" (nonburnished) samples effectively rules out mechanical factors such as Hertzian contact pressure as the primary cause. The only shared factor across all trials is the thermal history imposed by the EHLA process. It is, therefore, concluded that cyclic reheating, induced by the rotational motion during deposition, facilitates near-surface stress relaxation and local microstructural evolution. This explains the neutral stress profile observed in the upper 300 $\mu$m, while the sharp reappearance of compressive stresses beyond this depth is attributed to the residual mechanical effect of simultaneous burnishing. The etched cross section in Fig. 3(c) provides a brief visual indication of the microstructural change happening at ~300 $\mu$m depth attributed to this secondary HAZ. Remarkably, simultaneous burnishing promotes slightly deeper compressive stress penetration than sequential treatment, pointing toward an enhanced thermal–mechanical coupling effect unique to the simultaneous process suggested by the authors. The reason this discontinuity appears exclusively in the axial residual stress profile, while being absent in the circumferential direction, remains unclear. Further study is required to explain this behavior.

## IV. CONCLUSION

Within this study, the feasibility of the SCaRB process as a method of enhancing surface and subsurface properties of EHLA-deposited material was successfully demonstrated. Across the investigated parameter range, significant improvements were observed in surface finish, microhardness, and residual stress distribution. The integration of roller burnishing into the EHLA process introduces an additional degree of process control, above all through variation of the TCP offset Δz, enabling tailored adjustment of material properties to meet specific performance requirements.

With regard to surface finish, the presence of residual heat during simultaneous processing contributes to improved surface plasticity, enhancing the effectiveness of roller burnishing in reducing surface roughness. Interestingly, the most favorable results—both visually and as quantified by white light interferometry, were achieved at a moderate tool offset of $\Delta z = 4$ mm. This suggests that an optimal thermal window exists, beyond which excessive heat may reduce the effectiveness of surface smoothing.

The authors were surprised to discover that the largest increase in surface hardness was achieved through simultaneous roller burnishing at the lowest tool offset ($\Delta z = 1$ mm), significantly outperforming the other evaluated strategies. This enhancement may result from precold deformation effects, wherein mechanically induced strain facilitates grain refinement and cementite redistribution prior to thermal exposure, a phenomenon supported by research from Jia *et al.*,[20] that was shown to improve hardness and wear resistance of martensitic steel while maintaining its toughness. Furthermore, the interaction between deformation and elevated temperature may induce partial stress-induced transformation to martensite even above the $M_S$ temperature, leading to a higher final martensite content after rapid cooling.[21] In summary, the demonstrated effects open new opportunities for optimizing the surface integrity of EHLA coatings, particularly in terms of hardness and wear resistance, by leveraging simultaneous mechanical treatment during deposition.

In the context of landing gear repair, the ability of SCaRB to modify EHLA-induced residual stress states is of particular relevance. The results demonstrate that, while "as deposited" EHLA repair volumes exhibit pronounced tensile residual stresses beneath the surface—conditions known to compromise fatigue performance—all applied roller burnishing strategies successfully mitigated these stresses. Several processing conditions resulted in a complete transformation of tensile into compressive residual stresses, a modification that is well-documented to improve the bending fatigue performance of structural components.[11] Previous studies[22] have shown that compressive residual stresses introduced at elevated temperatures, particularly in the range of 250–300 °C, exhibit increased thermal and mechanical stability and contribute to enhanced fatigue strength and component longevity. Given that the residual heat from the EHLA process falls within a comparable temperature range, it is reasonable to anticipate similar beneficial effects when simultaneous roller burnishing strategies are employed.

As a proxy for residual thermal input from the EHLA process, the TCP offset proves to be a key parameter, enabling control over both the magnitude and depth distribution of compressive residual stresses, while also enabling intentional differentiation between axial and circumferential stress states. Such control supports strategic engineering of stress profiles to enhance structural integrity and fatigue performance. As such, the proposed SCaRB method presents an opportunity to optimize performance and safety in repaired components, with the potential to not only restore but enhance mechanical integrity beyond original specifications. Future research will be essential to fully exploit these capabilities.

## V. OUTLOOK

This study represents an initial investigation into the fundamental principles of simultaneous coating and roller burnishing. To provide further understanding of the complex process mechanics and to enable its practical adoption in the repair of safety-critical components and other demanding industrial applications, further systematic investigations are necessary.

In addition to the selected key parameters evaluated in this study, several other factors are expected to have a significant effect on the material properties after SCaRB processing. These include the applied burnishing force, the rotational speed of the workpiece, and the axial feed rate of both burnishing and EHLA tools.

Moreover, the current investigation was limited to two discrete values of TCP offset. To develop a more comprehensive understanding of the process behavior and the interaction between thermal and mechanical effects, future studies should explore a broader range of offset distances with finer gradation. In this context, a more detailed investigation of microstructural evolution under varying process conditions is essential. Electron backscatter diffraction analysis can be used to evaluate grain morphology, crystallographic texture, and phase transformations associated with simultaneous processing.

A key future step involves linking the various stress profiles generated by SCaRB to actual fatigue performance. This requires a dedicated fatigue testing campaign using test specimens processed with distinct burnishing strategies. The resulting data set would help identify optimal residual stress states and validate whether compressive stresses introduced during simultaneous processing deliver improved mechanical stability under servicelike conditions.

## ACKNOWLEDGMENTS

The presented research was supported within the framework of the "6th National Civil Aviation Research Programme (LuFo VI-3)" by the Federal Ministry for Economic Affairs and Energy on the basis of a decision by the German Bundestag (Grant No. 20Y2205E).

## AUTHOR DECLARATIONS

### Conflict of Interest

The authors have no conflicts to disclose.

### Author Contributions

**Viktor Glushych:** Conceptualization (lead); Data curation (equal); Formal analysis (lead); Funding acquisition (lead); Investigation (equal); Methodology (equal); Project administration (equal); Resources (lead); Supervision (equal); Visualization (equal); Writing – original draft (lead); Writing – review & editing (lead). **Kim Kallies:** Conceptualization (equal); Formal analysis (supporting); Investigation (equal); Methodology (equal); Project administration (equal); Writing – review & editing (equal). **Max Zimmermann:** Conceptualization (supporting); Methodology (supporting); Visualization (supporting). **Harald Betsch:** Conceptualization (equal); Investigation (supporting); Methodology (equal); Writing – review & editing (equal). **Bodo Vieland:** Conceptualization (supporting); Formal analysis (supporting); Methodology (supporting); Writing – review & editing (equal). **Christian Henk:** Conceptualization (supporting); Formal analysis (supporting); Investigation (supporting); Methodology (supporting); Writing – review & editing (equal). **Thomas Schopphoven:** Funding acquisition (equal); Resources (equal); Supervision (supporting). **Wilhelm Meiners:** Conceptualization (supporting); Methodology (supporting); Writing – review & editing (equal).

## REFERENCES

[1]Y. Liang, Z. Y. Liao, L. L. Zhang, M. W. Cai, X. S. Wei, and J. Shen, "A review on coatings deposited by extreme high-speed laser cladding: Processes, materials, and properties," Opt. Laser Technol. **164**, 109472 (2023).
[2]L. Zhou, G. Ma, H. Zhao, H. Mou, J. Xu, W. Wang, Z. Xing, Y. Li, W. Guo, and H. Wang, "Research status and prospect of extreme high-speed laser cladding technology," Opt. Laser Technol. **168**, 109800 (2024).
[3]V. Glushych, N. Dall, M. Zimmermann, T. Schopphoven, W. Meiners, and C. L. Häfner, "Fundamentals of simultaneous machining and coating (SMaC) through combination of extreme high-speed laser material deposition (EHLA) and turning," J. Laser Appl. **36**, 042037 (2024).
[4]P. Delgado, I. I. Cuesta, J. M. Alegre, and A. Díaz, "State of the art of deep rolling," Precis. Eng. **46**, 1–10 (2016).
[5]P. A. Ghodake, "Effect of burnishing process on behavior of engineering materials—A review," IOSR J. Mech. Civil Eng. **5**, 9–20 (2013).
[6]B. Denkena, T. Grove, B. Breidenstein, A. Abrão, and K. Meyer, "Correlation between process load and deep rolling induced residual stress profiles," Procedia CIRP **78**, 161–165 (2018).
[7]T. Pertoll, C. Buzzi, M. Leitner, and L. Boronkai, "Application of local fatigue strength approach to assess and optimise the impact of deep rolling on the fatigue performance of railway axles," Int. J. Fatigue **185**, 108335 (2024).
[8]J. T. Maximov, G. V. Duncheva, A. P. Anchev, and V. P. Dunchev, "Slide burnishing versus deep rolling—A comparative analysis," Int. J. Adv. Manuf. Technol. **110**, 1923–1939 (2020).
[9]W. J. Whitney and B. E. Schwab, "Crankshaft surfaces: Finishing methods, surface characterization and their influence on wear," Wear **108**, 345–356 (1986).
[10]W. W. Maxwell, B. R. Dudley, A. B. Cleary, J. Richards, and J. Shaw, "Measures to counter fatigue failure in railway axles," J. Inst. Locomot. Eng. **58**, 136–171 (1968).
[11]D. Hornbach and P. Prevéy, "Reducing corrosion fatigue and SCC failures in 300 M steel landing gear using low plasticity burnishing," in *SAE Technical Paper Series* (SAE International, Warrendale, PA, 2007).
[12]H. Liu, B. Wang, P. Chen, D. Li, J. Hao, H. Yang, X. He, and G. Yu, "Hierarchical heterogeneous microstructure for enhanced wear resistance of CoCrFeMnNi high-entropy alloy coatings via in-situ rolling assisted laser cladding," J. Manuf. Process. **141**, 105–120 (2025).
[13]K. Deng, A. P. Ompusunggu, Y. Xu, M. Skote, and Y. Zhao, "A review of material-related mechanical failures and load monitoring-based structural health monitoring (SHM) technologies in aircraft landing gear," Aerospace **12**, 266 (2025).
[14]A. Armaan, S. Keshav, and G. Srinivas, "A step towards safety: Material failure analysis of landing gear," Mater. Today Proc. **27**, 402–409 (2020).
[15]A-5B Gears, Struts and Couplings Committee, *AIR5885 Landing Gear Common Repair* (SAE International, Warrendale, PA, 2015).
[16]T. Li, L. Zhang, G. Chen, T. Schopphoven, A. Gasser, and R. Poprawe, "Eigenstrain reconstruction of residual stress and its application in extreme high-speed laser material deposition," J. Manuf. Process. **85**, 1054–1065 (2023).
[17]Q. Yan, K. Yang, Z. D. Wang, M. Z. Chen, G. F. Sun, and Z. H. Ni, "Surface roughness optimization and high-temperature wear performance of H13 coating fabricated by extreme high-speed laser cladding," Opt. Laser Technol. **149**, 107823 (2022).
[18]T. Li, L. Zhang, G. G. P. Bultel, T. Schopphoven, A. Gasser, J. H. Schleifenbaum, and R. Poprawe, "Extreme high-speed laser material deposition (EHLA) of AISI 4340 steel," Coatings **9**, 778 (2019).
[19]A. A. Somatkar, R. Dwivedi, and S. S. Chinchanikar, "Enhancing surface integrity and quality through roller burnishing: A comprehensive review of parameters optimization, and applications," Commun. Appl. Nonlinear Anal. **31**, 151–169 (2024).
[20]D. Jia, C. Zhang, R. Dong, H. Zhang, X. Gao, X. Feng, Z. Yang, and F. Zhang, "Driving martensitic transformation through pre-cold deformation: Unveiling the mechanism of microstructural evolution in martensite bearing steel," Mater. Des. **252**, 113788 (2025).
[21]K. Kanetani, T. Moronaga, T. Hara, and K. Ushioda, "Deformation-induced martensitic transformation behavior of retained austenite during rolling contact in carburized SAE4320 steel," ISIJ Int. **61**, 2629–2635 (2021).
[22]A. Cherif, H. Hochbein, W. Zinn, and B. Scholtes, "Increase of fatigue strength and lifetime by deep rolling at elevated temperature of notched specimens made of steel SAE 4140," HTM J. Heat Treat. Mater. **66**, 342–348 (2011).